Preprints of the 21st IFAC World Congress (Virtual)
Berlin, Germany, July 12-17, 2020

An Adaptive Disturbance Rejection Controller for Artificial Pancreas

Deheng Cai [*] **Wei Liu** [**] **Eyal Dassau** [***]
Francis J. Doyle III [***] **Xiaoling Cai** [**] **Junzheng Wang** [*]
Linong Ji [**] **Dawei Shi** [*]

[*] *State Key Laboratory of Intelligent Control and Decision of Complex Systems, School of Automation, Beijing Institute of Technology, Beijing 100081, China (e-mail: daweishi@bit.edu.cn).*
[**] *Department of Endocrine and Metabolism, Peking University People's Hospital, Beijing, China.*
[***] *Harvard John A. Paulson School of Engineering and Applied Sciences, Harvard University, Cambridge, MA 02138, USA.*

Abstract: Artificial pancreas (AP) systems are designed to automate glucose management for patients with type 1 diabetes. In this work, we propose an adaptive disturbance rejection control approach for AP systems to achieve safe and effective glucose regulation. The controller is built within the framework of active disturbance rejection control, but incorporates safety operation constraints, and glucose- and velocity-dependent parameter adaptation modules for the key control parameters. *In silico* performance comparison between the proposed controller and an adaptive zone model predictive controller (MPC) (Shi, Dassau, and Doyle III, 2019a) is conducted on the 10-adult cohort of the FDA-accepted UVA/Padova T1DM simulator. For both announced and unannounced meals, the controller achieves comparable glucose regulation performance in terms of mean glucose (134.9 mg/dL vs. 135.4 mg/dL, $p < 0.001$; 149.7 mg/dL vs. 151.7 mg/dL, $p < 0.001$, respectively) and percentage time in [70, 180] mg/dL (93.8% vs. 92.4%, $p < 0.001$; 76.0% vs. 72.4%, $p < 0.001$, respectively) without increasing the risk of hypoglycemia. The results indicate the feasibility of achieving comparable glucose regulation performance through a non-optimization control law for AP systems.

Keywords: Artificial pancreas, Active disturbance rejection control, Adaptive control, Glucose regulation.

1. INTRODUCTION

People with type 1 diabetes mellitues (T1DM) suffer from impaired glucose regulation that can cause chronic health problems, e.g., retinopathy and nephropathy (Diabetes Control and Complications Trial Research Group (1993)). With the technologies of continuous glucose monitoring (CGM) and continuous subcutaneous insulin infusion (CSII), artificial pancreas (AP) systems provide a promising way to improve health outcomes for patients with T1DM through automated insulin delivery. The performance of an AP relies on its feedback control algorithm, which adjusts insulin doses according to real-time CGM readings.

AP control algorithm design has drawn much research attention in the recent years (Doyle III et al., 2014; Thabit and Hovorka, 2016; Haidar, 2016). The main approaches include proportional-integral-differentiation (PID) control and model predictive control (MPC) (Steil (2013); Bequette (2013)). PID control was argued to have the ability of emulating the pancreatic β-cell insulin response (Steil et al. (2003)), and different PID-based AP algorithms have been evaluated in clinical studies (Steil et al. (2006); Garg et al. (2017)). Utilizing the knowlegde of plateaus phenomenon of pancreatic beta cell response after sustained hyperglycemia, Gopakumaran et al. (2005) proposed a fading memory PD control (FMPD) method. To improve the safety of the algorithms, Steil et al. (2011) proposed a PID control algorithm by incorporating an insulin feedback term for AP systems to avoid controller-induced hypoglycemia. To prevent hypoglycemia caused by insulin overdelivery, a PID control algorithm with insulin on board (IOB) constraints was proposed in Rossetti et al. (2017).

MPC determines the optimal insulin infusion of each control cycle by optimizing the dynamic glucose regulation performance while explicitly enforcing safety constraints. In recent years, MPC-based AP algorithms have been extensively investigated and evaluated in different clinical trials (Hovorka et al. (2010); Thabit et al. (2015)). Utilizing a compartment model determined by a Bayesian parameter estimation approach, Hovorka et al. (2004) proposed an MPC with safety constraints on insulin injection doses. Based on clinical experience, Toffanin et al. (2013) introduced an unconstrained MPC algorithm with multiple safety constraints designed. Since euglycemia is defined as a range of blood glucose (BG) values (e.g. 70-180 mg/dL), Doyle, Dassau and co-authors (Grosman et al. (2011); Gondhalekar et al. (2016, 2018)) developed a zone MPC approach featuring a diurnal zone cost function, IOB

constraints, velocity-weighting and velocity penalty; in a recent update of zone MPC, Shi et al. (2018, 2019a) introduced control penalty adaptation based on glucose and velocity information. Detailed discussions on the design considerations and developments of AP control algorithms can be found in Doyle III et al. (2014) and Shi et al. (2019b).

The move of developing home-use-safe wearable AP systems calls for low-complexity, reliable, and efficient control algorithms. In this work, we introduce a design that simultaneously bears the performance and flexibility of MPC for AP and the simplicity of a PID controller. Our controller is designed on the basis of an active disturbance rejection control (ADRC) structure, which can be understood as a generalization of the classic PID control. The main contribution of our work is the development of glucose- and velocity-dependent adaptation laws for the key parameters that determine the response of the proposed controller, which is motivated by the adaptive zone MPC design in Shi, Dassau, and Doyle III (2019a). Note that glucose and velocity-dependent switching mechanisms were also adopted in designing fuzzy logic controllers (FLC) for AP (Atlas et al., 2010; Richard et al., 2013; Mauseth et al., 2010); however, our work focus on characterizing different controller operation modes and building explicit ADRC parameter adaptation laws for each of these modes based on glucose and velocity information, whereas FLC encodes clinician expertise to develop a pre-determined dosing matrix corresponding to all possible combinations of glucose, velocity and even acceleration (Richard et al. (2013)). For safety considerations, we also enforce constraints on the maximum allowable insulin infusion rate and IOB in the controller design.

The performance of the proposed controller is evaluated through the 10-adult cohort of the US Food and Drug Administration (FDA) accepted Universities of Virginia (UVA)/Padova T1DM simulator (Dalla Man et al., 2014). Compared with the adaptive zone MPC introduced in Shi et al. (2019a), the proposed controller achieves comparable and satisfactory performance in terms of mean glucose level and percentage time in euglycemia for both announced and unannounced meals, without increasing the risk of hypoglycemia.

2. CONTROLLER STRUCTURE DESIGN

In this section, we present the structure of the proposed controller (see Fig. 1). The controller is built within the framework of ADRC, which inherits the simple error-driven structure of PID control, but incorporates a state observer to possess anti-disturbance capacity (Han, 2009; Yi and Zhao, 2014). Specifically, ADRC treats the total effect of model-plant mismatch and external disturbances as an additional state of the system, which is the so-called extended state, and compensates it in the control law design.

The proposed controller assumes a *virtual* nonlinear insulin-glucose model, which is obtained around the subject-specific time-dependent basal insulin infusion rate u_{b} that virtually corresponds to a steady-state glucose level G_{b}:

$$\ddot{G} = f(G, \dot{G}, d(t), t) + bu, \tag{1}$$
$$y = G, \tag{2}$$

where $u = u_{\mathrm{I}} - u_{\mathrm{b}}$ and $G = G_{\mathrm{BG}} - G_{\mathrm{b}}$ are the input and output of the model, respectively, u_{I} is the absolute insulin infusion rate, G_{BG} is the subject's BG value, $d(t)$ represents the disturbance introduced by the meals, exercise or other unmeasured effects, b denotes the input gain in the form of $b = \Delta b + b_0$, with b_0 representing the nominal gain selected as $b_0 = -k/u_{\mathrm{TDI}}$ and Δb being the uncertain part, and u_{TDI} denotes the subject specific total daily insulin amount. Note that the exact knowledge of $f(\cdot)$ is not needed in controller design and that the model in (1) is consistent with the structure of the control relevant model introduced in van Heusden et al. (2012). The key components of the proposed controller are described in the following subsections.

2.1 Tracking differentiator

A tracking differentiator (TDIFF) extracts the differential signal from a given noise-corrupted signal (Han (2009); Guo and Zhao (2013)), and has been adopted in a wide range of engineering applications (Zhang et al. (2019); Zhao et al. (2019)). Here, TDIFF calculates the glucose estimate $y_1(i)$, the glucose prediction $y_2(i)$, and the approximate differential signal $v_2(i)$ (namely, glucose velocity) Specifically, the TDIFF module utilized in the controller has the form

$$f_{\mathrm{h}}(i) = f_{\mathrm{han}}(v_1(i) - \mathrm{CGM}(i), v_2(i), r_1, h_0), \tag{3}$$
$$v_1(i+1) = v_1(i) + Tv_2(i), \tag{4}$$
$$v_2(i+1) = v_2(i) + Tf_{\mathrm{h}}(i), \tag{5}$$
$$y_1(i) = v_1(i+1) + \epsilon_1 v_2(i+1), \tag{6}$$
$$y_2(i) = v_1(i+1) + \epsilon_2 v_2(i+1), \tag{7}$$

where $T := 5$ [min] is sampling period, r_1 determines the tracking speed, h_0 is a filter coefficient, ϵ_1 and ϵ_2 are compensation coefficients satifying $\epsilon_2 > \epsilon_1 > 0$, and $f_{\mathrm{han}}(\cdot)$ denotes a time-optimal control synthesis function that enables fast tracking of the targeted CGM signal without overshoot (see Appendix A for the definition and Section III.A of Han (2009) for the detailed explanations). Generally, $v_1(i)$ is a tracking signal of CGM(i); to help compensate the phase delay and amplitude decay, the glucose estimate $y_1(i)$ of CGM(i) and glucose prediction $y_2(i)$ are calculated using the differential signal $v_2(i)$. The detailed design of ϵ_1, ϵ_2, r_1 and h_0 is discussed in Section 3.3.

2.2 Extended state observer

An extended state observer (ESO) is ultilized in ADRC to estimate the effect of the model-plant mismatch and external disturbances, which is compensated in the control law design. Denoting $x_1 := G$ and $x_2 := \dot{G}$, we define an extended state of the model in (1) and (2) as

$$x_3 := f(G, \dot{G}, d(t), t) + \Delta bu. \tag{8}$$

Based on this definition, a discrete-time ESO (Han, 2009) is designed:

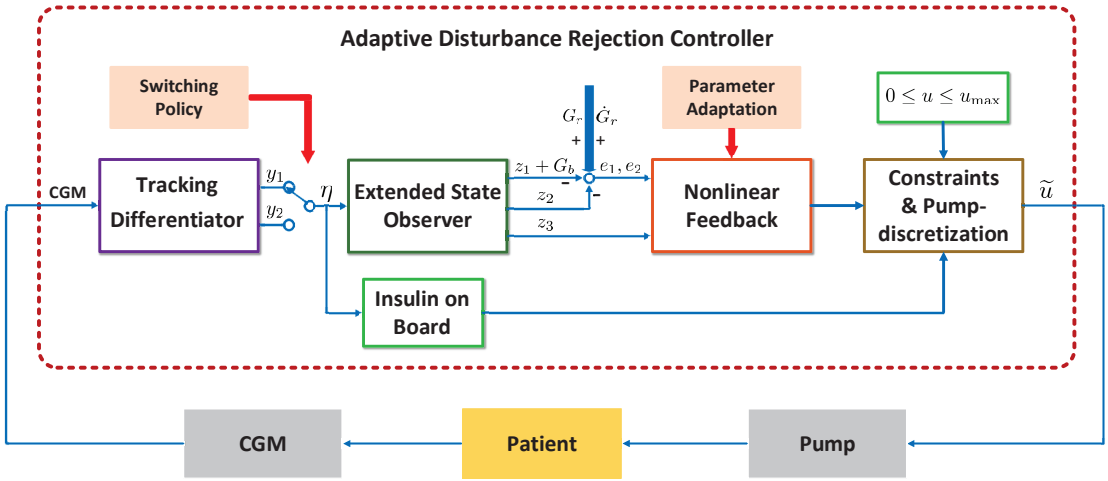

Fig. 1. Schematic of the proposed controller. The basic ADRC modules include a tracking differentiator, an extended state observer and a nonlinear feedback module. To ensure the safety of the controller, IOB constraints and upper/lower limits for insulin infusion are incorporated. To enable different controller behavior in ascending and descending BG situations, adaptation mechanisms are designed for ESO, IOB and nonlinear feedback (see Section 3 for details).

$$e(i) = z_1(i) - (\eta(i) - G_{\rm b}), \tag{9}$$
$$f_2(i) = f_e(e(i), \sigma_1, \mu),\ \ f_3(i) = f_e(e(i), \sigma_2, \mu), \tag{10}$$
$$z_1(i+1) = z_1(i) + T(z_2(i) - \lambda_1 e(i)), \tag{11}$$
$$z_2(i+1) = z_2(i) + T(z_3(i) + b_0 u(i) - \lambda_2 f_2(i)), \tag{12}$$
$$z_3(i+1) = z_3(i) + T(-\lambda_3 f_3(i)), \tag{13}$$

where z_1 and z_2 correspond to the estimates of x_1 and x_2, respectively, z_3 is the estimate of extended state x_3, and η is either the glucose estimate y_1 or the glucose prediction y_2 determined by a condition to be discussed in Section 3.1. Here σ_1 and σ_2 are design parameters, λ_1, λ_2 and λ_3 are the observer gains, and the function $f_e(\cdot)$ has the form

$$f_e(e, \sigma, \mu) = \begin{cases} \frac{e}{\mu^{1-\sigma}}, & |e| \le \mu, \\ |e|^{\sigma}\text{sign}(e), & |e| > \mu. \end{cases} \tag{14}$$

Parameter design will be discussed in Section 3.2.

2.3 Nonlinear feedback

To improve the closed-loop control performance, ADRC usually employs a nonlinear feedback control law (Yi and Zhao (2014)). With the state estimates provided by ESO, we consider the following feedback control law:

$$u(i) = (-u_0(i) - z_3(i))/b_0, \tag{15}$$
$$u_0(i) = f_{\rm han}(k_1 e_1(i), k_2 e_2(i), r, \varepsilon), \tag{16}$$
$$e_1 = G_{\rm r} - (z_1 + G_{\rm b}),\ \ e_2 = \dot{G}_{\rm r} - z_2, \tag{17}$$

where $G_{\rm r}$ and $\dot{G}_{\rm r}$ are the reference values of blood glucose and its rate of change, respectively, and k_1, k_2, r and ε are positive controller adaptation parameters. The design of these parameters will be discussed in Section 3.2. Note that the term $-z_3(i)$ in (15) is used to compensate the total disturbances at step i, so that the transfer function from $u_0(i)$ to $G(i)$ (c.f., equation (1)) will be approximately two cascaded integrators in discrete time (Yi and Zhao, 2014). In this regard, u_0 is designed in the form of $f_{\rm han}(\cdot)$, which is the time-optimal control synthesis function for two cascaded discrete-time integrators.

2.4 Safety constraints

To ensure the safety of the controller, several constraints at each step i are implemented. The first type of constraint provides upper and lower limits for the insulin infusion rate:

$$0 \le u(i)T + \frac{u_{\rm b}(i)T}{60\ \text{min/h}} \le u_{\max}, \tag{18}$$

where $u_{\max} := 0.5$ [U] denotes an upper bound on the bolus size. From (18), the minimum value of $u(i)$ is set to $-\frac{u_{\rm b}(i)}{60\ \text{min/h}}$, since the insulin-glucose system is a positive system.

IOB constraints based on insulin delivery history help prevent over-bolus when much insulin has been recently delivered. A revised IOB constraint based on the version used in Gondhalekar et al. (2018) is adopted in the controller. Let

$$\tau(\eta) := \max\{\min\{-\eta/30 + 12, 8\}, 2\}, \tag{19}$$

where the design of η is presented in Section 3.1. In particular, the IOB constraint employs IOB decay curves of length $\tau(\eta)$ based on either the estimated CGM y_1 or CGM prediction y_2, instead of only the current CGM level in Gondhalekar et al. (2018). The motivation for this is discussed in Section 3.1. At each step i, the IOB constraint is given as

$$u(i)T \le \overline{u}_{\rm IOB}(i), \tag{20}$$
$$\overline{u}_{\rm IOB}(i) := \max\{\Gamma(i) - \Phi(i),\ 0\}, \tag{21}$$

where $\Phi(i) \in \mathbb{R}$ is the estimated IOB based on the IOB decay curves at time step i determined by $\tau(\eta)$, and $\Gamma(i) \in \mathbb{R}$ is the required IOB at time step i depending on the current $\eta(i)$. The detailed calculation of $\Phi(i)$ and $\Gamma(i)$ can be found in Gondhalekar et al. (2018). Note that $\overline{u}_{\rm IOB}(i) = 0$ implies the controller is allowed to deliver no more than the basal rate $u_{\rm b}(i)T$.

2.5 Pump-discretization

Similar to Gondhalekar et al. (2016), as a CSII pump has a delivery resolution of δ [U], the final absolute

insulin infusion $\widetilde{u}(i)$ commanded to the pump is calculated according to a so-called carry-over module:

$$\widetilde{u}(i) := \delta \left\lfloor \frac{\hat{u}(i)}{\delta} \right\rfloor, \quad \hat{u}(i) := u(i)T + u_{\text{carry}}(i) + \frac{u_b(i)T}{60 \text{ min/h}},$$
$$u_{\text{carry}}(i) := \hat{u}(i-1) - \widetilde{u}(i-1) \geq 0, \quad u_{\text{carry}}(0) := 0,$$

where $\lfloor \cdot \rfloor$ denotes the floor operator, and $u(i)T$ is the control input at time step i after enforcing insulin delivery constraints and IOB constraints.

3. PARAMETER ADAPTATION FOR ADRC

In this section, adaptation mechanisms designed for the ESO, IOB and nonlinear feedback modules are presented, to enable different controller behavior for ascending and descending BG trajectories.

3.1 Adaptation of ESO and IOB

With the information of $y_1(i)$, $y_2(i)$ and $v_2(i)$ provided by TDIFF, a dynamic signal switching policy is proposed for $\eta(i)$ used in ESO and IOB, which has the following form:

$$\eta(i) := \begin{cases} y_2(i), \ y_1(i) > G_h, \ \text{sign}(v_2(i)) \geq 0, \\ y_2(i), \ y_1(i) < G_L, \ \text{sign}(v_2(i)) < 0, \\ y_1(i), \ \text{otherwise.} \end{cases} \tag{22}$$

Specifically, when the glucose is ascending and its measurement value is higher than a threshold G_h, or when the glucose is descending and its measurement value is lower than G_L, ESO and IOB will use the glucose prediction $y_2(i)$ to calculate their output signals, otherwise the glucose estimate $y_1(i)$ is used.

From (6) and (7), we observe that when the glucose level is steadily increasing, the predicted values are higher than the filtered values, which would introduce larger estimates z_1 and z_2 in (11) and (12), and lead to more responsive controller outputs. Meanwhile, the predicted values for ascending glucose traces would lead to shorter lengths of the IOB decay curves than the filtered values (c.f., equation (19)), which loosens the insulin infusion constraints. In this way, relatively more responsive controller behavior is encouraged when the glucose level is increasing towards hyperglycemia. Following this idea, a relatively more conservative insulin infusion policy will be observed for decreasing glucose traces towards hypoglycemia to ensure safety.

3.2 Parameter adaptation for nonlinear feedback

The behavior of nonlinear feedback module is determined by k_1, k_2, r and ε. To simplify the parameter design problem, we fix r and design ε, so that the following inequalities always hold

$$|n_1 + \varepsilon n_2| \leq \varepsilon^2 r, \ |n_2 + \frac{n_1 + \varepsilon n_2}{\varepsilon}| \leq \varepsilon r. \tag{23}$$

According to (A.4) in Appendix A, we can obtain a following linear approximate expression of $f_{\text{han}}(n_1, n_2, r, \varepsilon)$

$$f_{\text{han}}^{\text{approx}}(n_1, n_2, r, \varepsilon) = -\frac{2n_2 + n_1/\varepsilon}{\varepsilon}, \tag{24}$$

so that the control law in (15) can be approximated as

$$u(i) \approx \left((2k_2 e_2 + \frac{k_1 e_1}{\varepsilon})/\varepsilon - z_3(i) \right) / b_0. \tag{25}$$

From (25), we observe that ε is a coefficient that determines the overall aggressiveness of controller; a small value for ε will lead to aggressive controller responses and *vice versa*. On the other hand, k_1 and k_2 adjust the weights of the tracking error and its rate of change in control law, and thus determine the aggressiveness of controller with respect to glucose excursion and its rate of change, respectively.

To assist our design, we first introduce a basic function $f_a(x, \Upsilon)$ that is utilized to build the adaptation laws for ε, k_1 and k_2. Specifically, $f_a(x, \Upsilon)$ is designed as an exponential function with saturation:

$$f_a(x, \Upsilon) := \min\{a_1, \exp\{\alpha x^\beta\} + a_2 - 1\}, \quad x \geq 0, \tag{26}$$

where $\Upsilon := [a_1, a_2, \alpha, \beta]$ is a quadruple that determines the shape of this function. In particular, the maximum (saturation) and minimum values of the curve is determined by a_1 and a_2, respectively, and the steepness of the curve is controlled by α and β.

To achieve parameter adaptation, we define different scenarios based on the value and trend of glucose prediction. Specifically, when the glucose is ascending, we divide the glucose range into three regions based on the glucose estimate y_1 provided by TDIFF: 1) $y_1 \leq G_h$, 2) $G_h < y_1 < G_H$ and 3) $y_1 \geq G_H$. Similarly, when glucose is descending, we divide the glucose range into two regions: 1) $y_1 \geq G_L$ and 2) $y_1 < G_L$, respectively. Parameter adaptation laws are designed for each region as follows:

$$k_1 := \begin{cases} f_a(v_2, \Upsilon_1^{k_1}), & y_1 \leq G_h, \ \text{sign}(v_2) \geq 0, \\ b_1, & G_h < y_1 < G_H, \ \text{sign}(v_2) \geq 0, \\ b_1, & y_1 \geq G_H, \ \text{sign}(v_2) \geq 0, \\ b_2, & y_1 \geq G_L, \ \text{sign}(v_2) < 0, \\ b_3, & y_1 < G_L, \ \text{sign}(v_2) < 0, \end{cases}$$

$$k_2 := \begin{cases} f_a(v_2, \Upsilon_1^{k_2}), & y_1 \leq G_h, \ \text{sign}(v_2) \geq 0, \\ c_1, & G_h < y_1 < G_H, \ \text{sign}(v_2) \geq 0, \\ c_1, & y_1 \geq G_H, \ \text{sign}(v_2) \geq 0, \\ c_2, & y_1 \geq G_L, \ \text{sign}(v_2) < 0, \\ f_a(|v_2|, \Upsilon_2^{k_2}), & y_1 < G_L, \ \text{sign}(v_2) < 0, \end{cases}$$

$$\varepsilon := \begin{cases} f_a(G_h - y_1, \Upsilon_1^{\varepsilon}), & y_1 \leq G_h, \ \text{sign}(v_2) \geq 0, \\ A - f_a(G_H - y_1, \Upsilon_2^{\varepsilon}), & G_h < y_1 < G_H, \ \text{sign}(v_2) \geq 0, \\ d_1, & y_1 \geq G_H, \ \text{sign}(v_2) \geq 0, \\ d_2, & y_1 \geq G_L, \ \text{sign}(v_2) < 0, \\ d_2, & y_1 < G_L, \ \text{sign}(v_2) < 0, \end{cases} \tag{27}$$

where v_2 is the approximate differential signal of glucose measurement provided by TDIFF in (5) to determine whether the glucose is ascending or descending; b_1 is the maximum (saturation) value of $f_a(v_2, \Upsilon_1^{k_1})$, c_1 is the maximum (saturation) value of $f_a(v_2, \Upsilon_1^{k_2})$, c_2 is the minimum value of $f_a(|v_2|, \Upsilon_2^{k_2})$ and d_1 is the maximum (saturation) value of $f_a(G_H - y_1, \Upsilon_2^{\varepsilon})$; b_2, b_3 and d_2 are positive constants; A is the sum of maximum (saturation) and minimal values of $f_a(G_H - y_1, \Upsilon_2^{\varepsilon})$. The design principles for the adaptation laws in each region are presented in the following, and the design of the parameters is presented in Section 3.3.

Region 1) $y_1 \leq G_h$, $\text{sign}(v_2) \geq 0$: In this case, the controller should keep a conservative insulin delivery policy for robustness to the CGM noise to ensure safety.

Consequently, according to (25), k_1 and k_2 are designed to gradually increase with the increase of change rate of glucose value, and ε is designed to gradually decrease with the increase of glucose value to determine the overall aggressiveness of controller.

Region 2) $G_h < y_1 < G_H$, $\text{sign}(v_2) \geq 0$: This is a key region where the pump should deliver enough insulin to prevent early postprandial hyperglycemia so as to regulate the glucose level back into normal region as soon as possible. The controller is required to stay responsive until y_1 is approaching an upper threshold G_H to prevent postprandial hypoglycemia. To implement this principle, k_1 and k_2 take the maximum (saturation) value in $f_a(v_2, \Upsilon_1^{k_1})$ and $f_a(v_2, \Upsilon_1^{k_2})$, respectively, and ε is designed to increase when y_1 is approaching the upper threshold G_H.

Region 3) $y_1 \geq G_H$, $\text{sign}(v_2) \geq 0$: As discussed above, a suitably-designed controller would have delivered enough insulin in Region 2 so that only moderate insulin need to be delivered in this region. To do this, k_1 and k_2 still take the values in Region 2, and ε is set as the maximum (saturation) value in $f_a(G_H - y_1, \Upsilon_2^{\varepsilon})$.

Region 4) $y_1 \geq G_L$, $\text{sign}(v_2) < 0$: In this region, when the glucose is at a high level but is falling slowly, a moderate amount of insulin (above basal rate) could be delivered to alleviate hyperglycemia, but pump suspension should be adopted when glucose is falling rapidly. Based on this design principle, we assign constant values to ε, k_1 and k_2 so that the weight of the tracking error is lower than that of the glucose rate of change in the control law.

Region 5) $y_1 < G_L$, $\text{sign}(v_2) < 0$: When glucose is descending into this region, controller should be extremely conservative and sensitive to the change rate of glucose value to prevent over-delivery. To do this, ε still takes the value in Region 4, k_1 is fixed to a designed constant, and k_2 is designed to gradually increase with the increase of the absolute glucose velocity. Moreover, when glucose value y_1 is lower than threshold G_L, TDIFF provides glucose prediction values to both IOB and ESO, which will also make the controller to act conservatively.

3.3 Parameter design

The parameters of the proposed controller are designed and evaluated using virtual patients of the UVA/Padova T1DM metabolic simulator (Dalla Man et al. (2014)). The parameter design is performed using the "average patient" with an *in silico* protocol which starts from 7:00 with one meal of 60 g carbohydrate (CHO) at 9:00. The parameters are designed using a trial-and-error approach based on the glucose data obtained from the "average patient" for both announced and unannounced meals, so that satisfactory glucose regulation performance in terms of average glucose, percent time in [70, 180] mg/dL, and percent time below 70 mg/dL can be achieved. The obtained parameters are summarized in Tables 1-2. Meanwhile, the evaluation of the proposed control algorithm with the obtained parameters is conducted on the 10-patient cohort considering different scenarios. The results are reported in Section 4.

Note that the 12-hour protocol is used as a "test protocol" for controller design, and a different protocol with multiple meals of different amounts of CHOs is used as the "verification protocol" to evaluate the performance of the designed controller (see Section 4).

4. IN SILICO PERFORMANCE ANALYSIS

As mentioned above, the proposed controller is evaluated on the 10-adult cohort of the UVA/Padova simulator. For comparison purpose, the protocol designed in Shi et al. (2018) is introduced to evaluate the performance of controller. The protocol starts from 7:00 on Day one and lasts two days (48 hours) during which breakfast (50 g CHO), lunch (75 g CHO) and dinner (75 g CHO) are consumed at 8:00, 12:00 and 19:00, respectively.

The proposed controller is compared with the adaptive zone MPC controller introduced in Shi et al. (2019a) (denoted as "Control"). For both controllers, the pump resolution is selected as 0.05 [U]. Based on the introduced protocol, *in silico* experiments are performed on the whole 10-adult cohort using additive CGM noises (with random seeds 1-10), separately, under the scenarios of announced meals and unannounced meals, and thus a total of 100 simulations are performed for each scenario and each controller. Note that the results of the adaptive zone MPC reported in Shi et al. (2019a) were obtained on the 100-adult cohort, which is why the results reported here are slightly different. The results for the scenarios of announced meals and unannounced meals are presented in Sections 4.1 and 4.2, respectively. The statistical results are summarized in TABLE 3, and the performance of the proposed controller is illustrated in Figs. 2 and 3, where the 5%, 25%, 75% and 95% quartile curves together with the median curves are presented.

4.1 Announced meals

From TABLE 3, compared with the adaptive zone MPC, the proposed non-optimization-based controller achieves similar (and slightly improved) performance for glucose regulation with announced meals without increasing the risk of hyperglycemia (percent time < 70 mg/dL, 0.0% vs. 0.0%, $p = 0.441$). Satisfactory performance for hyperglycemia control is achieved, which is reflected in percent time in the euglycemic range of 70-180 mg/dL (93.8% vs. 92.4%, $p < 0.001$), mean glucose (134.9 mg/dl vs. 135.4 mg/dL, $p < 0.001$), hyperglycemia (percent time > 250 mg/dL, 0.0% vs. 0.0%, $p = 0.500$) and glucose variability (SD glucose, 25.8 vs. 28.2, $p < 0.001$). The discussions of controller performance are consistent with the quartile curves in Fig. 2.

4.2 Unannounced meals

Similar to the case of announced meals, the proposed controller achieves comparable performance to the adaptive zone MPC in terms of percent time in the euglycemic range of 70-180 mg/dL (76.0% vs. 72.4%, $p < 0.001$), mean glucose (149.7 mg/dl vs. 151.7 mg/dL, $p < 0.001$), hyperglycemia (percent time > 250 mg/dL, 1.0% vs. 1.2%, $p < 0.001$), and glucose variability (SD glucose, 43.0 vs. 44.9, $p < 0.001$). From Fig. 3, we can observe that the controller is able to reduce insulin infusion when the glucose concentration is rapidly decreasing to ensure safety. Again,

Table 1. Parameters for TDIFF and ESO

Parameters for nominal input gain and TDIFF	$b_0 = -6/u_{\mathrm{TDI}}$	$K_1 = 3$ (Filter signal)	$K_2 = 7$ (Glucose ascending ($y_1 > G_h$))
	$r_1 = 20$	$h_0 = 2T$	$K_2 = 5$ (Glucose descending ($y_1 < G_L$))
Parameters for ESO	$\lambda_1 = 1/T$	$\lambda_2 = 1/(2T^2)$	$\lambda_3 = 1/(160T^3)$
	$\sigma_1 = 0.5$	$\sigma_2 = 0.25$	$\mu = T$

In this table, T denotes sampling period, $G_h = 250$ mg/dL and $G_L = 135$ mg/dL.

Table 2. Parameters for nonlinear feedback

Glucose ascending ($G_h = 135$, $G_H = 250$)			Glucose descending ($G_L = 180$)		Other parameters
$y_1 \le G_h$	$G_h < y_1 < G_H$	$y_1 \ge G_H$	$y_1 \ge G_L$	$y_1 < G_L$	
$\Upsilon_1^{k_1} = \{0.01, 0.005, 0.01, 5\}$	$k_1 = 0.01$	$k_1 = 0.01$	$k_1 = 0.002$	$k_1 = 0.005$	$G_{\mathrm{r}} = 110$
$\Upsilon_1^{k_2} = \{0.05, 0.01, 0.01, 5\}$	$k_2 = 0.05$	$k_2 = 0.05$	$k_2 = 0.02$	$\Upsilon_2^{k_2} = \{0.1, 0.02, 0.002, 2\}$	$\dot{G}_{\mathrm{r}} = 0$
$\Upsilon_1^{\varepsilon} = \{25, 12, 0.35, 0.8\}$	$\Upsilon_2^{\varepsilon} = \{40, 12, 2, 0.5\}$	$\varepsilon = 40$	$\varepsilon = 8$	$\varepsilon = 8$	$r = 10$

Table 3. Metrics of glucose regulation for announced and unannounced meals

Scenario (#Simulations=100)	Announced meals			Unannounced meals		
Metric	Control	Proposed	p value	Control	Proposed	p value
% time						
<54 mg/dL	0.0 (0.0)	0.0 (0.0)	0.500	0.0 (0.0)	0.0 (0.0)	1.000
<70 mg/dL	0.0 (0.0)	0.0 (0.0)	0.441	0.0 (0.0)	0.0 (0.0)	0.211
70-180 mg/dL	92.4 (10.2)	**93.8 (9.2)**	**<0.001**	72.4 (13.4)	**76.0 (11.3)**	**<0.001**
>180 mg/dL	7.6 (10.0)	**6.2 (9.2)**	**<0.001**	27.6 (13.4)	**24.0 (11.0)**	**<0.001**
>250 mg/dL	0.0 (0.0)	0.0 (0.0)	0.500	1.2 (9.5)	**1.0 (7.9)**	**<0.001**
Mean glucose (mg/dL)	135.4 (6.1)	**134.9 (6.4)**	**<0.001**	151.7 (19.9)	**149.7 (16.8)**	**<0.001**
SD glucose (mg/dL)	28.2 (8.2)	**25.8 (4.8)**	**<0.001**	44.9 (14.1)	**43.0 (14.4)**	**<0.001**
Mean glucose at 07:00	121.0 (15.2)	**118.5 (17.0)**	**<0.001**	121 (15.5)	**113.0 (15.2)**	**<0.001**

Data in this table are shown as median (inter quartile range). Statistically significant ($p < 0.05$) changes are highlighted in bold.

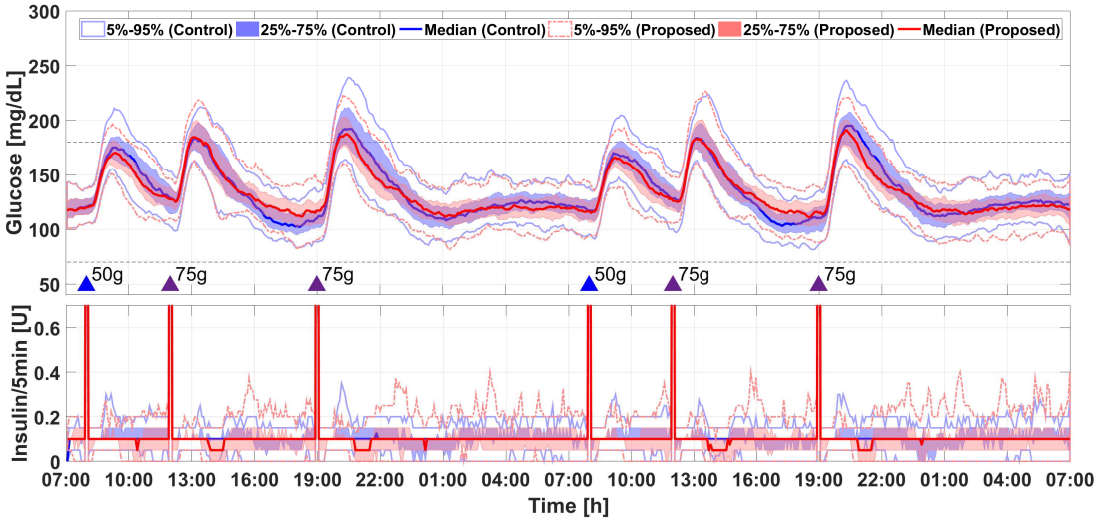

Fig. 2. Performance comparison for announced meals in terms of glucose regulation and insulin delivery. Blue and purple triangles denote meals of 50 g and 75 g CHO, respectively.

no increased risk of hypoglycemia is observed (percent time < 70 mg/dL, 0.0% vs. 0.0%, $p = 0.211$).

5. CONCLUSION

In this work, an adaptive ADRC controller is proposed for closed-loop glucose regulation. The proposed non-optimization-based controller is able to responsively command insulin when blood glucose is rapidly increasing above the euglycemic range, and safely turn off or turn down insulin infusion when the glucose is low or rapidly decreasing. The effectiveness and robustness of the controller is evaluated on the 10-adult cohort of the UVA/Padova simulator through comparisons with the adaptive zone MPC in Shi et al. (2019a). In our next step, clinical studies are planned to further test the performance of the proposed control algorithm.

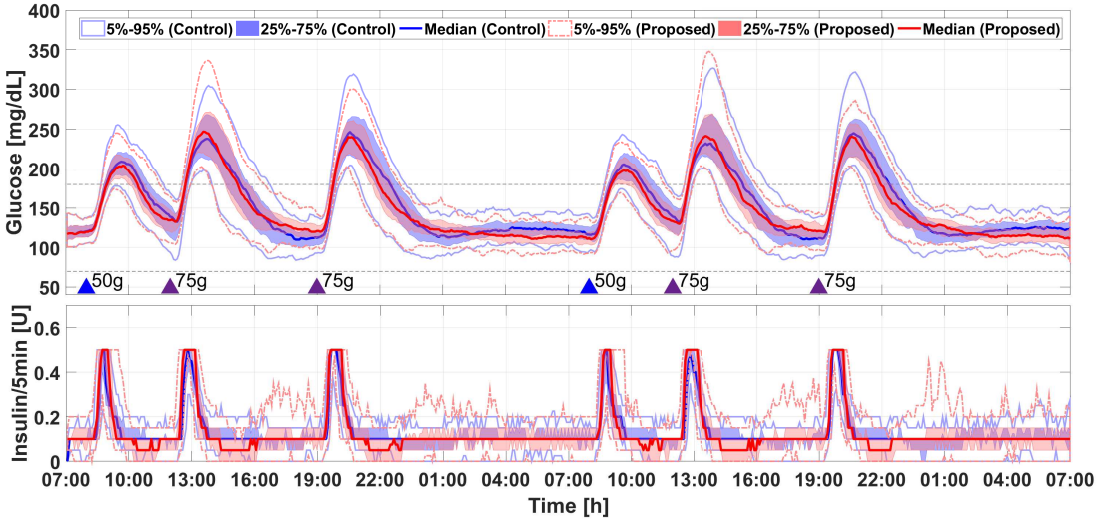

Fig. 3. Performance comparison for unannounced meals in terms of glucose regulation and insulin delivery. Blue and purple triangles denote meals of 50 g and 75 g CHO, respectively.

ACKNOWLEDGEMENTS

This work was supported in part by the Beijing Natural Science Foundation under Grant 4192052 and in part by the National Natural Science Foundation of China under Grant 61973030. Access to the distributed version of the University of Virginia (UVA)/Padova metabolic simulator for research purposes under a license agreement between the Epsilon Group Analytics and the Beijing Institute of Technology is acknowledged.

REFERENCES

Atlas, E., Nimri, R., Miller, S., Grunberg, E.A., and Phillip, M. (2010). MD-logic artificial pancreas system: A pilot study in adults with type 1 diabetes. *Diabetes Care*, 33(5), 1072–1076.

Bequette, B.W. (2013). Algorithms for a closed-loop artificial pancreas: The case for model predictive control. *J. Diabetes Sci. Technol.*, 7(6), 1632–1643.

Dalla Man, C., Micheletto, F., Lv, D., Breton, M., Kovatchev, B., and Cobelli, C. (2014). The UVA/PADOVA type 1 diabetes simulator: new features. *J. Diabetes Sci. Technol.*, 8(1), 26–34.

Diabetes Control and Complications Trial Research Group (1993). The effect of intensive treatment of diabetes on the development and progression of long-term complications in insulin-dependent diabetes mellitus. *N. Engl. J. Med.*, 1993(329), 977–986.

Doyle III, F.J., Huyett, L.M., Lee, J.B., Zisser, H.C., and Dassau, E. (2014). Closed-loop artificial pancreas systems: engineering the algorithms. *Diabetes care*, 37(5), 1191–1197.

Garg, S.K., Weinzimer, S.A., Tamborlane, W.V., Buckingham, B.A., Bode, B.W., Bailey, T.S., Brazg, R.L., Ilany, J., Slover, R.H., Anderson, S.M., Bergenstal, R.M., Grosman, B., Roy, A., Cordero, T.L., Shin, J., Lee, S.W., and Kaufman, F.R. (2017). Glucose outcomes with the in-home use of a hybrid closed-loop insulin delivery system in adolescents and adults with type 1 diabetes. *Diabetes Technol. Ther.*, 19(3), 155–163.

Gondhalekar, R., Dassau, E., and Doyle III, F.J. (2016). Periodic zone-MPC with asymmetric costs for outpatient-ready safety of an artificial pancreas to treat type 1 diabetes. *Automatica*, 71, 237–246.

Gondhalekar, R., Dassau, E., and Doyle III, F.J. (2018). Velocity-weighting & velocity-penalty MPC of an artificial pancreas: Improved safety & performance. *Automatica*, 91, 105 – 117.

Gopakumaran, B., Duman, H.M., Overholser, D.P., Federiuk, I.F., Quinn, M.J., Wood, M.D., and Ward, W.K. (2005). A novel insulin delivery algorithm in rats with type 1 diabetes: The fading memory proportional-derivative method. *Artif. Organs*, 29(8), 599–607.

Grosman, B., Dassau, E., Zisser, H., Jovanovič, L., and Doyle III, F.J. (2011). Multi-zone-MPC: Clinical inspired control algorithm for the artificial pancreas. In *Proc. 18th IFAC World Congr.*, 7120 – 7125.

Guo, B. and Zhao, Z. (2013). Weak convergence of nonlinear high-gain tracking differentiator. *IEEE Trans. Autom. Control*, 58(4), 1074–1080.

Haidar, A. (2016). The artificial pancreas: How closed-loop control is revolutionizing diabetes. *IEEE Control Syst. Mag.*, 36(5), 28–47.

Han, J. (2009). From PID to active disturbance rejection control. *IEEE Trans. Ind. Electron.*, 56(3), 900–906.

Hovorka, R., Allen, J.M., Elleri, D., Chassin, L.J., Harris, J., Xing, D., Kollman, C., Hovorka, T., Larsen, A.M.F., Nodale, M., Palma, A.D., Wilinska, M.E., Acerini, C.L., and Dunger, D.B. (2010). Manual closed-loop insulin delivery in children and adolescents with type 1 diabetes: a phase 2 randomised crossover trial. *The Lancet*, 375(9716), 743–751.

Hovorka, R., Canonico, V., Chassin, L.J., Haueter, U., Massi-Benedetti, M., Federici, M.O., Pieber, T.R., Schaller, H.C., Schaupp, L., Vering, T., and Wilinska, M.E. (2004). Nonlinear model predictive control of glucose concentration in subjects with type 1 diabetes. *Physiol. Meas.*, 25(4), 905–920.

Mauseth, R., Wang, Y., Dassau, E., Jr, R.K., Matheson, D., and Zisser, H. (2010). Proposed clinical application

for tuning fuzzy logic controller of artificial pancreas utilizing a personalization factor. *J. Diabetes Sci. Technol.*, 4(4), 913–922.

Richard, M., Hirsch, I.B., Jennifer, B., Robert, K., Don, M., Srinath, S., and Carla, G. (2013). Use of a "fuzzy logic" controller in a closed-loop artificial pancreas. *Diabetes Technol. Ther.*, 15(8), 628–633.

Rossetti, P., Quirós, C., Moscardó, V., Comas, A., Giménez, M., Ampudia-Blasco, F.J., León, F., Montaser, E., Conget, I., Bondia, J., and Vehí, J. (2017). Closed-loop control of postprandial glycemia using an insulin-on-board limitation through continuous action on glucose target. *Diabetes Technol. Ther.*, 19(6), 355–362.

Shi, D., Dassau, E., and Doyle III, F.J. (2019a). Adaptive zone model predictive control of artificial pancreas based on glucose and velocity-dependent control penalties. *IEEE Trans. Biomed. Eng.*, 66(4), 1045–1054.

Shi, D., Dassau, E., and Doyle III, F.J. (2018). Zone model predictive control with glucose- and velocity-dependent control penalty adaptation for an artificial pancreas. In *Proc. Amer. Control Conf.*

Shi, D., Deshpande, S., Dassau, E., and Doyle III, F.J. (2019b). Chapter 1 - feedback control algorithms for automated glucose management in t1dm: the state of the art. In R.S. Sanchez-Pena and D.R. Chernavvsky (eds.), *The Artificial Pancreas*, 1 – 27. Academic Press.

Steil, G.M. (2013). Algorithms for a closed-loop artificial pancreas: The case for proportional-integral-derivative control. *J. Diabetes Sci. Technol.*, 7(6), 1621–1631.

Steil, G.M., Palerm, C.C., Kurtz, N., Voskanyan, G., Roy, A., Paz, S., and Kandeel, F.R. (2011). The effect of insulin feedback on closed loop glucose control. *J. Clin. Endocrinol. Metab.*, 96(5), 1402–1408.

Steil, G.M., Rebrin, K., Darwin, C., Hariri, F., and Saad, M.F. (2006). Feasibility of automating insulin delivery for the treatment of type 1 diabetes. *Diabetes*, 55(12), 3344–3350.

Steil, G.M., Rebrin, K., Janowski, R., Darwin, C., and Saad, M.F. (2003). Modeling β-cell insulin secretion - implications for closed-loop glucose homeostasis. *Diabetes Technol. Ther.*, 5(6), 953–964.

Thabit, H. and Hovorka, R. (2016). Coming of age: The artificial pancreas for type 1 diabetes. *Diabetologia*, 59(9), 1795–1805.

Thabit, H., Tauschmann, M., Allen, J.M., Leelarathna, L., Hartnell, S., Wilinska, M.E., Acerini, C.L., Dellweg, S., Benesch, C., Heinemann, L., Mader, J.K., Holzer, M., Kojzar, H., Exall, J., Yong, J., Pichierri, J., Barnard, K.D., Kollman, C., Cheng, P., Hindmarsh, P.C., Campbell, F.M., Arnolds, S., Pieber, T.R., Evans, M.L., Dunger, D.B., and Hovorka, R. (2015). Home use of an artificial beta cell in type 1 diabetes. *N. Engl. J. Med.*, 373(22), 2129–2140.

Toffanin, C., Messori, M., Palma, F.D., Nicolao, G.D., Cobelli, C., and Magni, L. (2013). Artificial pancreas: Model predictive control design from clinical experience. *J. Diabetes Sci. Technol.*, 7(6), 1470–1483.

van Heusden, K., Dassau, E., Zisser, H.C., Seborg, D.E., and Doyle III, F.J. (2012). Control-relevant models for glucose control using a priori patient characteristics. *IEEE Trans. Biomed. Eng.*, 59(7), 1839–1849.

Yi, H. and Zhao, C. (2014). Active disturbance rejection control: Methodology and theoretical analysis. *ISA Trans.*, 53(4), 963–976.

Zhang, H., Xie, Y., Xiao, G., Zhai, C., and Long, Z. (2019). A simple discrete-time tracking differentiator and its application to speed and position detection system for a maglev train. *IEEE Trans. Control Syst. Technol.*, 27(4), 1728–1734.

Zhao, L., Cheng, H., Zhang, J., and Xia, Y. (2019). Angle attitude control for a 2-DOF parallel mechanism of PMAs using tracking differentiators. *IEEE Trans. Ind. Electron.*, 66(11), 8659–8669.

Appendix A. TIME-OPTIMAL CONTROL SYNTHESIS FUNCTION

In this appendix, the function $f_{\rm han}(n_1, n_2, r, \varepsilon)$ is introduced, which was named after the inventor of this function and is mathematically defined as

$$\begin{cases} d = r\varepsilon^2,\ a_0 = \varepsilon n_2,\ y = n_1 + a_0, \\ a_1 = \sqrt{d(d+8|y|)}, \\ a_2 = a_0 + \text{sign}(y)(a_1 - d)/2, \\ s_y = (\text{sign}(y+d) - \text{sign}(y-d))/2, \\ a = (a_0 + y - a_2)s_y + a_2, \\ s_a = (\text{sign}(a+d) - \text{sign}(a-d))/2, \\ f_{\rm han} = -r(\frac{a}{d} - \text{sign}(a))s_a - r\text{sign}(a). \end{cases} \tag{A.1}$$

As mentioned earlier, this function is a time-optimal control synthesis function for the discrete-time stabilization of two integrators in cascade with bounded input (Han (2009)):

$$n_1(i+1) = n_1(i) + Tn_2(i), \tag{A.2}$$

$$n_2(i+1) = n_2(i) + Tu,\ |u| \le r, \tag{A.3}$$

where T is the sampling period, and u is the control law. Letting v be a desired tracking signal, we can obtain the time-optimal discrete-time TDIFF in Section 2.1 using $f_{\rm han}(n_1 - v, n_2, r, \varepsilon)$. A rigorous proof on the convergence of the TDIFF is provided in Guo and Zhao (2013).

Besides, a linear approximate expression $f^{\rm a}_{\rm han}(\cdot)$ of $f_{\rm han}(\cdot)$ in (A.1) was explored in the literature, which has the form of

$$\begin{cases} q = n_1 + \varepsilon n_2, \\ p = n_2 + \frac{q}{\varepsilon}, \\ m = n_1 + \frac{\varepsilon}{2}n_2 + \frac{|n_2|n_2}{2r}, \\ f^{\rm a}_{\rm han} = -r\text{sat}(p, \varepsilon r), \quad |p| \le \varepsilon r \text{ and } |q| \le \varepsilon^2 r, \\ f^{\rm a}_{\rm han} = -r\text{sign}(m), \quad \text{otherwise.} \end{cases} \tag{A.4}$$

where $\text{sat}(p, \varepsilon r)$ is a linear saturation function defined as

$$\text{sat}(p, \varepsilon r) = \begin{cases} \text{sign}(p), & |p| > \varepsilon r, \\ \frac{p}{\varepsilon r}, & |p| \le \varepsilon r. \end{cases} \tag{A.5}$$

This approximate function is used and analyzed in the parameter design of our work.